Materials and Structures (2022) 55:175
https://doi.org/10.1617/s11527-022-02014-7

ORIGINAL ARTICLE

Durability aspects of concretes made with boron-activated high belite cement (HBC)

Guler Fakhraddin Muhyaddin · Diler Sabah Asaad

Received: 4 May 2022 / Accepted: 27 July 2022

Abstract Boron-activated high belite cement could be a promising alternative to ordinary Portland cement to provide considerable energy savings and to reduce the environmental impacts of concrete production. However, this material has little practical use in industry without satisfactory durability, which is a fundamental feature of serviceable concrete structures subjected to working conditions. Experimental research was conducted to ascertain the durability of the concretes made with boron-stabilized high belite cement (HBC) over that of ordinary cement (OPC)-based concretes. Four concrete mixtures were designed with HBC and OPC at 0.35 and 0.55 w/c ratios. Apart from early and late compressive and tensile strengths, the durability of the concretes was tested for free and restrained shrinkage, water and chloride ion permeability, and accelerated corrosion resistance. Test results revealed that the concretes with HBC demonstrated outstanding durability performance than compared to OPC-concrete in many aspects owing to its high belite content leading to much less calcium hydroxide, thus providing a denser matrix and interface in the concrete.

Keywords Boron · Belite rich cement · Durability · Shrinkage cracking · Corrosion · Permeability

G. F. Muhyaddin (✉) · D. S. Asaad
Construction and Materials Technology Department, Erbil Polytechnic University, Erbil, Iraq
e-mail: guler.muhyaddin@epu.edu.iq

Published online: 05 August 2022

1 Introduction

The United Nations has been bringing together countries for the worldwide climate summits called COPs (Conference of the Parties) for almost three decades for the environmental protection of the world. The COP21 event was organized in Paris in 2015, where the participants promised to be involved in cooperation to reduce global warming to below 2 °C and aim for 1.5 degrees. Moreover, COP26, which took place in Glasgow, Scotland in 2021, revealed that greenhouse gas emissions must be halved by the next decade and that carbon emissions need to be zero by the middle of this century if the global temperature rise is to be limited to 1.5 °C [1]. Therefore, reducing carbon emissions and preserving natural resources have been the goals of many industries and studies [2–4].

In contrast to the aims of the Paris Agreement, a high content of $CaCO_3$ in raw mixtures of ordinary Portland cement causes a substantial amount of CO_2 release to the atmosphere during the manufacturing process. Moreover, it requires a large amount of energy before and after production in preparing the raw materials as well as in grinding the clinkers. It is known that one ton of OPC production results in 0.97 tons of CO_2 emissions, being the sum of electrical power, decarbonation, and thermal power. Therefore, cement manufacturing plants constitute approximately 7–8% of the overall CO_2 emissions in the world [5–8]. The manufacture of cement expends

40–50% of its total CO_2 emissions for production, 20–30% for thermal energy, and 12–15% for electrical energy [9, 10]. In light of these facts, the development of more sustainable cement with lower CO_2 emissions has received great attention from cement and concrete researchers [8]. Among the main compounds of the ordinary Portland cement clinker that generate a large amount of CO_2, alite (C_3S) is reported to be the most responsible phase. Thus, increasing the belite (C_2S) phase accompanied by a decrease in the alite phase leads to a great reduction in CO_2, which has been accomplished by using industrial byproducts with significant lime, silica, and alumina contents [11, 12].

As an environmentally friendly material, research on belite cement has attracted significant attention from scientists [13–18]. To find a worldwide use, however, the activation of such cements has become a research priority because of their slow hydraulic reaction resulting in lower strength development at early ages [19, 20]. According to Cuesta et al. [20], activation of the belite cement can be obtained by three methods, namely, chemical, physical, and admixture activation. Kachimi et al. [15] investigated the cooling rate of belite clinker by water quenching to stabilize the reactive belite so that the clinker had improved hydraulic properties. Adding NaF and Fe_2O_3 contributed to the properties of the clinker burned at low temperature. Cuberos et al. [16] attempted to enhance the early age mechanical strength of high belite cement. For this, the slow hydraulic reactivity of belite phases, which led to low early strength, was activated by alkaline oxides. In the study of Martin-Sodeno et al. [17], belite sulfoaluminate (BSA) cement was introduced as an alternative to OPC. Three types of BSA cements differing in the main compositions C_2S, $C_4A_3\$$ (also called Clein's salt), CA, and $C_{12}A_7$ were obtained under laboratory conditions, where C, S, A, and \$ designate CaO, SiO_2, Al_2O_3, and SO_3, respectively. Fifteen minutes at 1350 °C was sufficient for good clinkering. Londono-Zuluaga et al. [18] produced belite-alite-ye'elimite (BAY) cement, which was activated by the presence of both alite and ye'elimite to overcome low early strength. BAY cement led to mortars with higher compressive strengths. Cements with a high belite content have a denser crystalline structure and higher thermodynamic stability, which are the main reasons for their low hydraulic reactivity [21]. As a good measure to remedy the low reactivity of belite with water, the use of nanomineral admixtures was proposed to accelerate the hydration reaction [22, 23]. Carbon dioxide curing was also considered in recent studies to enhance the belite reaction [24–27].

According to previous studies, enhanced hydraulic reactivity of the belite phase could be achieved by incorporating a stabilizer oxide, such as boron oxide (B_2O_3) [28, 29]. For this, boron ions are introduced into the lattice structure of C_2S to stabilize its α'- and β-polymorphs because the α'-C_2S phase is more active than β–C_2S [28, 30]. As a result, the hydraulically nonreactive γ-form does not form at all. Preventing γ formation is so important because when the β-belite transforms to the γ belite, a volume change occurs, which in turn causes disintegration (dusting effect) [31, 32]. Koumpouri and Angelopoulos [33] investigated the possibility of belite cement production with low energy consumption by adding boron oxide. For this, belite cements with three kinds with boron waste and boric acid were made and tested. Belite cement was produced by using boron oxide. Moreover, the delay in the compressive strength of such cements was found to be more affected by the crystal type of the belite rather than its content in the clinker. In the study by Saglik et al. [34], belite-rich cement was produced by adding Colami Colemanite ore, in which CaO, B_2O_3 and SiO_2 are the main compounds; the final product was called boron-modified active belite (BAB) cement, abbreviated as "BAB-cement". Typically, the alite (C_3S) phase, one of the principal compounds of OPC, was much less abundant in the boron-activated belite-rich cement. Indeed, the author stated that it was not produced at all in the BAB cement. Therefore, it was quite rich in the active and stable belite phase found in the structural form of α-C_2S or α'-C_2S. The burning temperature in the rotary kiln was well below 1325 °C, which in turn provided a 25% reduction in CO_2 emissions during its manufacturing stage.

Although researchers have paid significant attention to the activation of belite-rich cement, the literature on mortar and concrete made with such cement is very limited. Sirtoli et al. [35] investigated the variation in the volume stability of concretes with calcium sulfoaluminate (CSA) cement, which partially replaced PC. Shrinkage and creep were tested and observed to be lower than those of the PC mortar. Sui et al. [36] attempted to produce 50–80 MPa high strength concretes using high belite cement and fly ash

at low w/c ratios. The resultant concretes at 90 days reached 116 MPa, which even passed that of ordinary PC concrete with 110 MPa. In the study of Afroughsabet et al. [37], the mechanical and physical performance of calcium sulfoaluminate (CSA) cement-based concretes was examined. It was observed that replacing OPC with CSA cement enhanced the mechanical properties. Using CSA cement reduced the shrinkage but raised the risk of corrosion. Guerrero et al. [38] hydrothermally activated fly ash and CaO at 200 °C to manufacture fly ash-belite cement to be used in making mortars. The durability of the mortars was examined in a sulfated medium via flexural strength. It was observed that the decreased porosity and pore size distribution densified the structure so that the flexural strength increased. Gokce [39] studied the high-temperature resistance of OPC and boron-activated belite cement mortars exposed to 900 °C. Mortar made with boron-activated belite cement was less resistant to high temperature than PC mortar.

As is extensively observed in the literature, concretes with high belite cement are based on the use of calcium sulfoaluminate (CSA) cement, although boron has been emphasized as a very good activator in the fabrication of sustainable high active belite cements (HBCs). As mentioned above, the production of such cement may decrease CO_2 release by as much as 25%, but they are of little practical application unless the concrete with HBC is sufficiently durable in aggressive environments [40]. However, few studies have been conducted on the durability of HBC-based concretes, such as drying and autogenous shrinkage, restrained shrinkage cracking, water and chloride ion permeability, and corrosion performance of the reinforcing bars embedded in the concrete. Saglik [41] stated that the heat of hydration produced by the BAB-cement was quite low at early ages and substantially decreased the adiabatic temperature rise of concrete when compared to that of OPC. The concretes made with BAB-cement also had lower water permeability. Irico et al. [42] investigated the durability of concrete made with high belite cement (HBC). It was reported that HBC-incorporated concretes demonstrated good resistance to freeze–thaw scaling and an extraordinary ability to resist chloride ion penetration. Both Saglik [41] and Irico et al. [42] strongly proposed incorporating such cements in mass concrete production, as it has a very low heat of hydration. Based on this property of HBC, Irico et al. [43] suggested its use to produce high-performance self-compacting concretes (SCCs) as an alternative to OPC because the high cement content in SCC mixtures generates a high degree of heat of hydration. Thus, SCCs made with high belite cement had reduced heat development and longer service life.

2 Experimental details

2.1 Materials

Boron-activated high belite cement (HBC) obtained from the Goltas cement manufacturing plant in Denizli, Turkey and CEM I 42.5R ordinary Portland cement (OPC) conforming to Turkish standard TS EN 197-1 [44] were used in the concrete mixtures. The physical and chemical properties of both HBC and OPC are presented in Table 1. Fine aggregate was a mixture of river sand and natural sand, whereas crushed limestone with a maximum particle size of 22 mm was used as coarse aggregate. A superplasticizer based on sulfonated naphthalene formaldehyde with a specific gravity of 1.22 was used to achieve consistent workability.

2.2 Concrete mixture proportioning, casting and curing of test specimens

Two concrete series were designed at water/cement ratios of 0.35 (low w/c) and 0.55 (high w/c). High belite cement and ordinary Portland cement were incorporated into both of the concrete mixtures with cement contents of 450 and 350 kg/m^3, respectively (Table 2). Aggregate grading was kept constant for the concretes at each w/c ratio. Superplasticizer was added during mixing to achieve the workability specified by a slump of 15 $\pm$ 2 cm. The mixtures were designated based on the cement type and the w/c ratio so that HBC-0.35 indicates concrete made with high belite cement at a w/c of 0.35.

A power-driven revolving pan was used to mix all of the concretes. First, dry concrete ingredients were mixed for one minute; thereafter, the water-containing superplasticizer was added for an additional three minutes. The following samples were cast from each mixture: eighteen 150 mm cubes for compression, six 150 $\times$ 300 mm cylinders for splitting tension, eight 100 $\times$ 200 mm cylinders for sorptivity and chloride

Table 1 Properties of ordinary portland cement (OPC) and boron activated high-belite- cement (HBC)

Item	OPC	HBC
Si02 (%)	19.73	19.10
Al203 (%)	5.09	4.68
Fe203 (%)	3.99	3.42
Ca0 (%)	62.86	57.10
Mg0 (%)	1.61	1.32
S03 (%)	2.62	2.68
Na20 (%)	0.18	0.34
K20 (%)	0.80	0.78
Cl^{-}(%)	0.01	0.001
B_2O_3 (%)		3.0
Insoluble residue (%)	0.24	0.20
Loss on ignition (%)	1.90	1.40
Free lime (%)	0.57	–
Specific gravity (g/cm^3)	3.14	3.15
Setting time, Vicat needle Initial/Final (h-min)	2-46/3-44	2-50/3-25
Le chatelier (mm)	1	1.5
Specific surface area (m^2/kg)	327	427

Table 2 Concrete mixture proportioning (kg/m^3)

w/c*	Cement	Water	Fine Aggregate		Coarse Aggregate		SP**
			CrushSand	Natural Sand	No I	No II	
0.35	450	157.5	94.0	747.2	644.4	366.5	4.1
0.55	350	192.5	90.5	736.5	631.8	360.5	2.8

*w/c: water/cement ratio;
**SP: Superplasticizer

ion permeation, four 100 × 200 mm cylinders with reinforcing bars for corrosion cracking, six 70 × 70 × 280 mm prisms for free and autogenous shrinkage, and two ring specimens for restrained shrinkage. All of the specimens were cast into the steel molds at least in two layers, compacted on a vibrating table. The samples, except for those for testing shrinkage, were covered with a plastic sheet and left in the casting room for one day. Thereafter, they were demolded and immersed in water until the testing age. Free, autogenous, and restrained shrinkage specimens were cured in a climate chamber at 20 °C and 100% relative humidity for 4 h and then demolded.

2.3 Measurement and testing

The compressive strength values of the concretes with HBC and OPC were tested at 1, 3, 7, 28, 56, and 90 days on three 150 mm cubes. Similarly, the splitting tensile strength was determined on Ø150 × 300 mm cylinders at 28 and 90 days. The tests were carried out as per ASTM C39 [45] and C496 [46] by means of a 2000 kN capacity testing machine.

Drying shrinkage was monitored according to ASTM C157 [47]. After demolding the concrete prisms, steel pins were glued on to fix the gage length of 200 mm, as shown in Fig. 1, and then they were dried for 60 days in a climate chamber at 23 ± 2 ^{0}C and 50 ± 5% relative humidity. Three specimens with dimensions of 70 × 70 × 280 mm were tested for each concrete type. Similarly, autogenous shrinkage of the concretes was measured on three 70 × 70 × 280 mm prisms. First, thin plastic sheets with two layers were entirely applied to the interior sides of the prisms prior to casting of the concrete. Next, the concrete was cast into molds, which were kept in a climate chamber at 20 °C and 100% relative humidity for approximately 4 h. After the steel pins adhered to the concrete surface, the sides of the molds were removed. Finally, the prism was entirely covered by another layer of plastic sheet and two layers of aluminum foil by means of adhesive tape (Fig. 2).

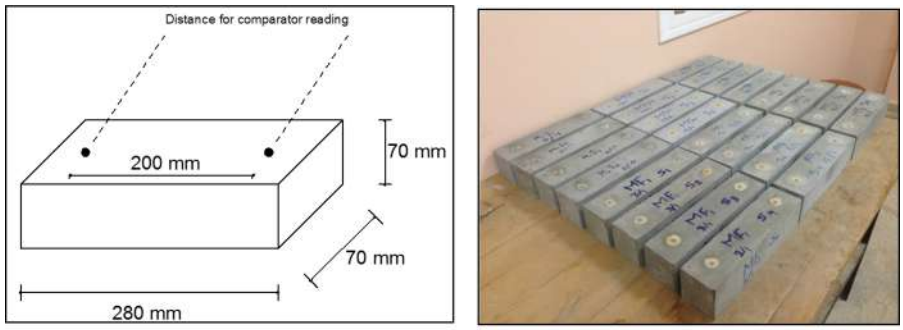

Fig. 1 **a** Measurement of shrinkage strain **b** Free shrinkage test specimens

Fig. 2 Preparing the specimens for autogenous deformation **a** Pre-sealing of specimens with two layers of plastic sheets **b** Final sealing of the specimens with a layer of aluminum foil

Then, they were maintained in a climate chamber at 20 ± 2 °C and 100 ± 5% relative humidity for 60 days. A dial gauge extensometer with a 200 mm gauge length and 0.002 strain accuracy was used to measure the length change.

Moreover, ring-type specimens were adopted to monitor the cracking of concrete induced by restrained shrinkage. Figure 3 shows a schematic view of such a ring and a photograph of a specimen equipped with a crack width measuring microscope. Upon drying, the concrete was exposed to an inner stress generated by the restraining effect of the interior steel ring. However, the tensile hoop stress measured on the concrete surface differs from that on the inner shell by as little as 10%. The highest radial stress was measured to be only one-fifth of the maximum hoop stress. When the steel ring restrains the shrinkage of concrete upon drying, the concrete annulus is subjected to an almost uniaxial tension. Additionally, a concrete thickness of 35 mm, one-fourth of its 140 mm width, was chosen to provide the concrete specimen with a uniform shrinkage throughout its width [48–51]. After stripping off the outer steel ring, the upper surface of the concrete was covered by silicon rubber to allow drying to occur solely from the outer surface. Eventually, the concrete annulus was subjected to drying at 23 ± 2 °C and 50 ± 5% relative humidity, conforming to ASTM C157 [47] over a period of 60 days, in the same way as the drying shrinkage specimens. Restrained shrinkage cracking on the ring specimens was monitored using a crack detecting microscope, as shown in Fig. 3b. For this, the microscope was fixed at the center of the base plate by means of a locator attached to a horizontal bar in such a way that it was possible to check the entire circumferential surface of the concrete. For each crack, three measurements (one

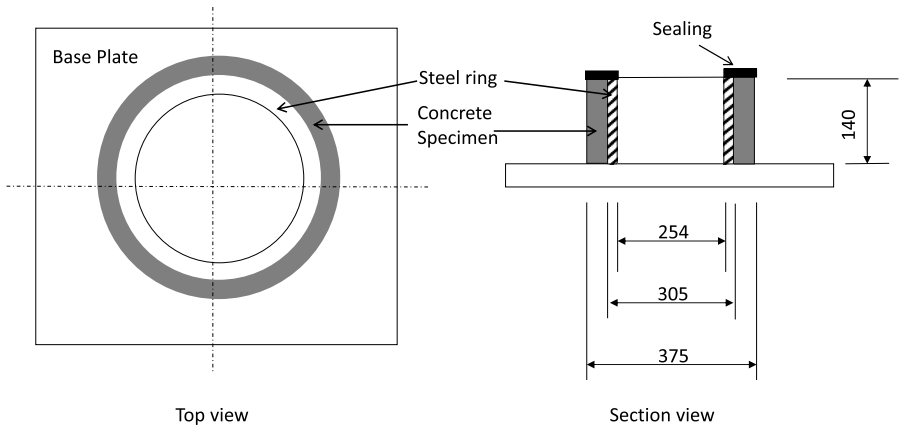

Fig. 3 Test setup for restrained shrinkage test: **a** schematic view, **b** photographic view

at the center and the other two at the centers of the top and bottom halves) were performed, and their average was reported as the crack width. The surface of the concrete ring was inspected daily for new cracks, and the width of a present crack was measured via the microscope.

The water rise through the capillary pores of the concretes was measured via a sorptivity test, which provides the rate at which water is drawn into the concrete pores. First, two Ø100 × 60 mm samples were cut out from the Ø100 × 200 cylinders and then maintained in an oven at 80 °C until a constant mass was measured. Next, they were kept in a sealed container to cool them to ambient temperature. To allow the free water rise to occur through only the bottom surface, the sides of the concrete samples were sealed by paraffin and then placed on glass rods in a testing tray (Fig. 4). The samples were brought into contact with water up to a height of 5 mm from the bottom surface. As an indication of water absorption, the increase in the sample mass was monitored by weighing the samples outside the tray every 1 h over a period of 24 h. Finally, the volume of absorbed water was computed by dividing the mass increase by the nominal surface area of the sample as well as by the density of water. The sorptivity coefficient, which accounts for the capillary water suction of the concrete, was then computed as the slope of the line best fitting a plot of the volume of the absorbed water versus the square root of time.

The resistance of the concretes to chloride ion penetration was determined via the RCPT (rapid chloride permeability test) in terms of charge passed through the concrete, as per ASTM C1202 [52]. Figure 5 shows the RCPT setup utilized in this study. A 50 mm thick disk sample was cut from the mid portions of the Ø100 × 200 mm cylinder with a saw. After being conditioned for moisture as described in ASTM C1202 [52], the disc was fixed between two cells of the test unit so that its one face was brought

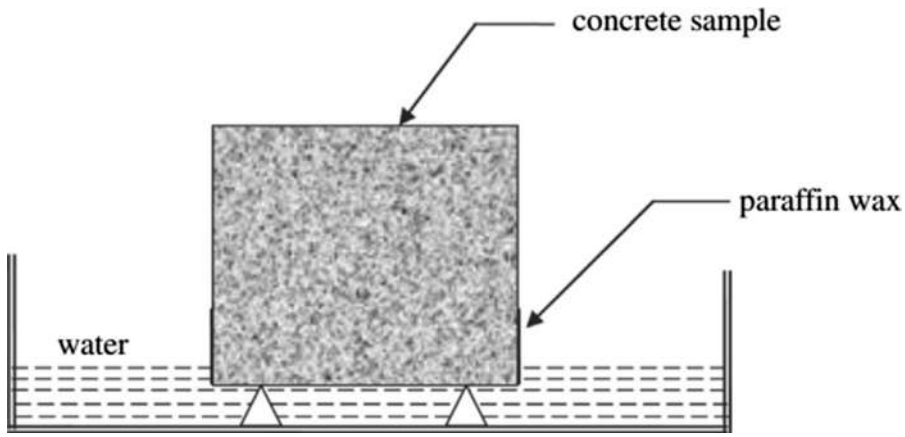

Fig. 4 Sorptivity measurement

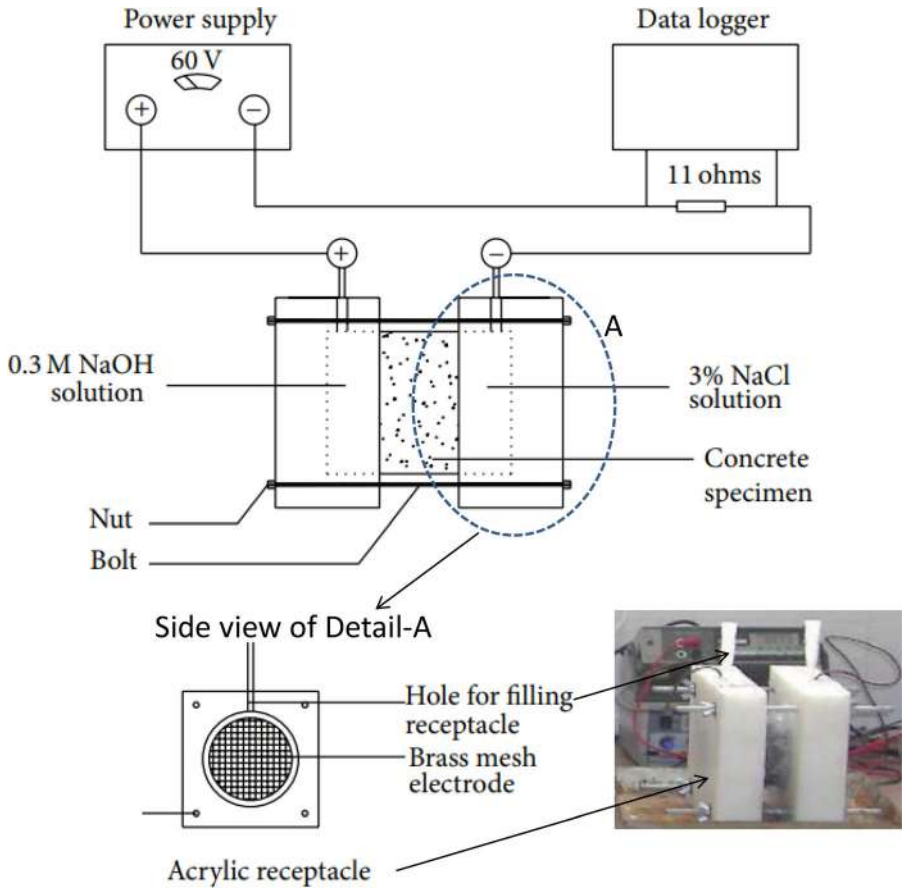

Fig. 5 Rapid chloride permeability measurement

into contact with 0.30 N NaOH, while the other face was in contact with 3% NaCl, as shown in the inset of Fig. 5. Thereafter, a 60.0 ± 0.1 V direct voltage was applied across the faces, and the current that passed through the concrete disk was recorded by a data acquisition system for 6 h. At the end of the test, the area under the current–time graph that accounts for the charge passed (in coulombs) was obtained. Two

specimens for each concrete were tested at 28 and 90 days.

An accelerated corrosion test was utilized to determine the corrosion performance of the concretes made with OPC and HBC. Figure 6a exhibits a schematic diagram of the corrosion cell in which the steel rebar, steel plates, and sodium chloride (NaCl) solution represent the anode, cathode, and electrolyte, respectively. The reinforced concrete cylinder was immersed in a 4% sodium chloride solution to half its height in a plexiglass tank. The steel bar embedded in the concrete cylinder as the working electrode was connected to the positive terminal of a power supply. As the counter electrode, the stainless steel plates located next to the concrete samples in the solution were connected to the negative terminal. To initiate the corrosion process, a power source of direct current supplied a 12 V anodic potential. As shown in Fig. 6b, there is an abrupt increase in the current as soon as corrosion cracks appear on the concrete surface. For

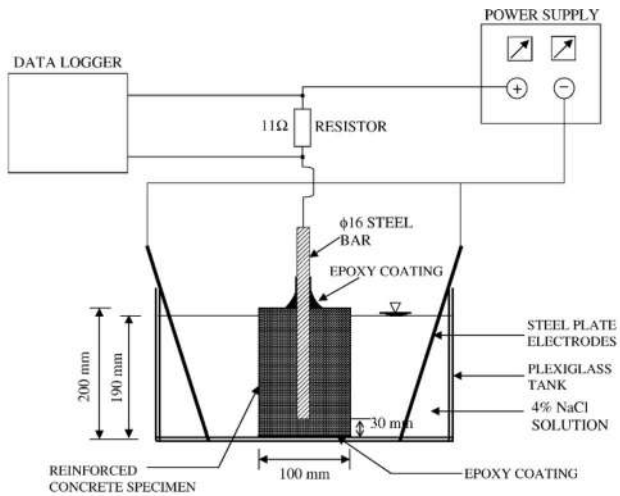

(a)

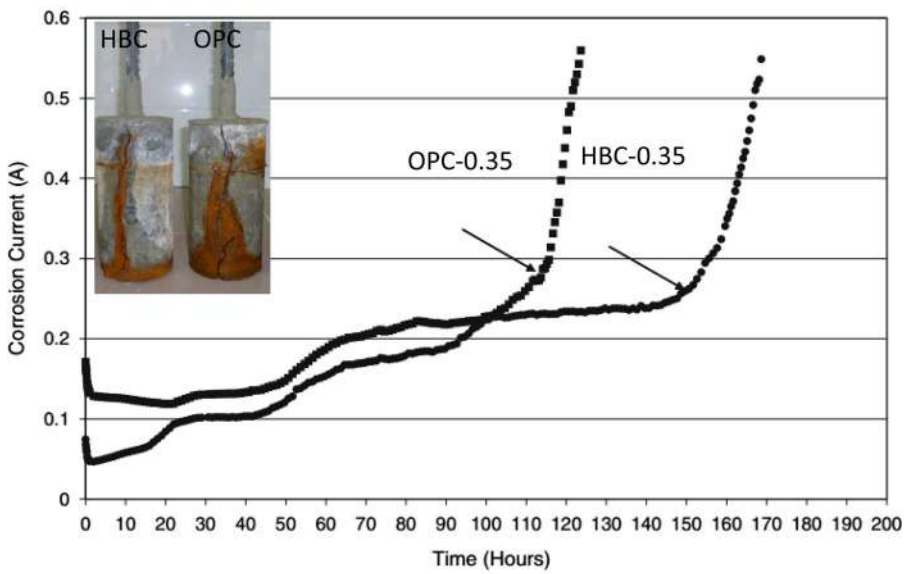

(b)

Fig. 6 Accelerated corrosion test setup **a** Schematic representation, **b** Typical corrosion cracking

this, the variation in the current with time was recorded continuously by a data logger until concrete failure. Two specimens for each mixture were tested at 28 and 90 days.

3 Results and discussions

3.1 Mechanical properties

The development of compressive strength and splitting tensile strength of the concretes with high belite cement (HBC) and ordinary Portland cement (OPC) are shown in Figs. 7 and 8, respectively. The large difference in the composition of the cements plays an important role in the strength of the concretes, especially at early ages. Figure 7 shows that the strength gain of the HBC concretes was much slower until 28 days of curing period compared to that of the OPC concretes, irrespective of the w/c ratio. Thus, the HBC concrete was said to have lower early strength. In the case of a low w/c ratio, the compressive strengths at 14 days were 63 and 70 MPa for the concretes with HBC and OPC, respectively. The corresponding strength values were 35 and 40 MPa, respectively. Figure 7 indicates a limiting curing age of 28 days for the HBC-based concretes. Indeed, they had lower compressive strength than OPC concretes until 28 days; thereafter, the strength gain was much faster in the case of the former. Irrespective of the w/c ratio, concretes with HBC surpassed the OPC-concretes at 28 days onward in terms of compressive strength. After 90 days of curing, the compressive strengths of the HBC and OPC concretes were measured to be 83 and 77 MPa at a low w/c ratio and 57 and 48 MPa at a high w/c ratio, respectively.

The splitting tensile strength of the concretes followed their compressive strength development at 28 and 90 days (Fig. 8). At both w/c ratios, HBC concretes had higher strength values than OPC concretes. From 28 to 90 days, the splitting tensile strength of the HBC increased from 3.39 to 4.27 and from 2.25 to 3.55 MPa at low and high w/c ratios, respectively. Such values indicate 26 and 57% improvements in the splitting tensile strength, respectively. However, these strength increments in the case of OPC-based concretes were almost 14 and 24%, respectively.

The remarkable rise in the long-term compressive and splitting tensile strengths of the concretes with HBC proved the presence of active belite as the main ingredient in the HBC. The HBC used in this study was composed of approximately 3.0% (wt.) B_2O_3 (boric oxide) as the main activator. Therefore, HBC has almost no C_3S, whereas it has an extremely high amount of active and stable α-C_2S as well as α'-C_2S crystal phases, which leads to the formation of a more packed and denser concrete microstructure [34]. In the

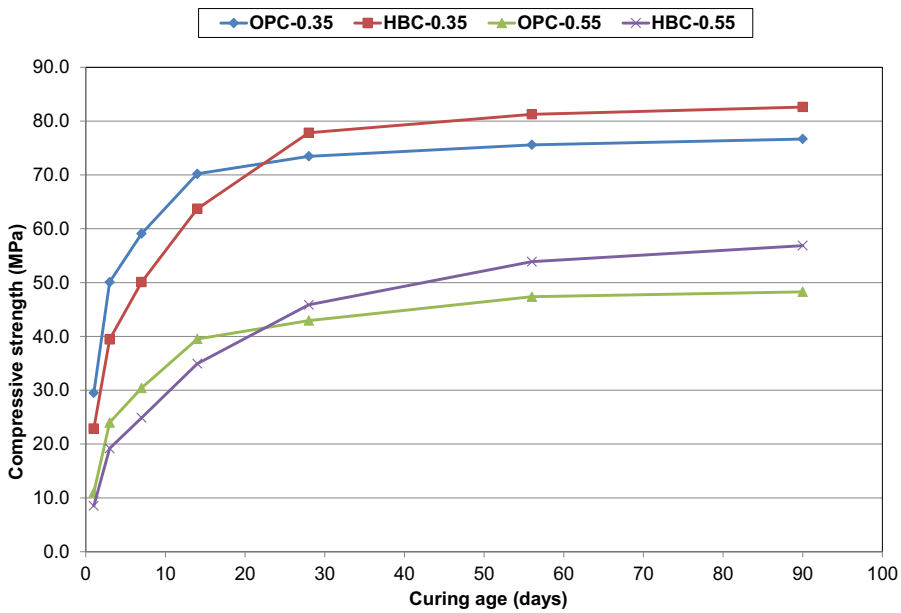

Fig. 7 Variation in the compressive strength with curing age

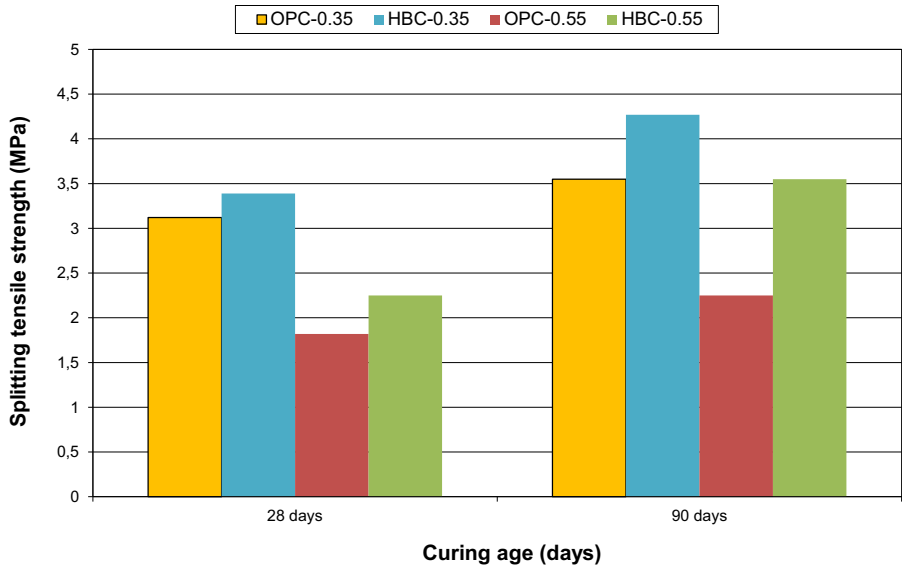

Fig. 8 Splitting tensile strength of the OPC or HBC-concretes

study by Sui et al. [36], the splitting tensile strength of the HBC-based concrete displayed a similar strength development pattern as the compressive strength with the curing period in terms of low early strength, comparable 28-day strength and high long-term strength compared with the OPC-based concrete.

3.2 Drying shrinkage, autogenous shrinkage, and restrained shrinkage induced cracking

The total shrinkage of concrete covers both drying and autogenous shrinkages. Loss of moisture to the atmosphere from the concrete when exposed to drying causes the former, while consumption of mixing water in the hydration process results in the latter [53, 54]. Over the hydration period of 60 days, the drying and autogenous shrinkage of the concretes with HBC and OPC are shown in Figs. 9 and 10, respectively. At the early ages, the OPC-concrete exhibited net shrinkage that occurred at a fast rate and continued over the hydration period. The ultimate shrinkages of the OPC-0.35 and OPC-0.55 mixtures were 0.0943% and 0.0742%, respectively. However, the counterpart concretes with HBC at the low and high w/c ratios had shrinkage of 0.0709% and 0.0510%, respectively, at 60 days. With the use of HBC in the concretes, the ultimate shrinkage development was much slower, and even HBC-0.35 concrete had a smaller shrinkage strain than OPC-0.55 concrete. Using HBC especially played a marked role in the early hydration period. At the end of six days, for instance, the concretes with HBC almost halved the shrinkage values for both low and high w/c ratios. Early stabilization of the shrinkage at later ages was also observed. As long as the effect of the w/c ratio was considered, both types of concretes exhibited similar behavior, such that a low w/c ratio caused higher shrinkage deformation mainly due to the presence of a high cement content.

The development of autogenous shrinkage for the HBC- and OPC-based concretes is illustrated in Fig. 10. The behavior of the concretes was similar to the drying shrinkage when the ultimate shrinkage is considered. The HBC-incorporated concretes suffered less autogenous shrinkage deformation than the concretes with OPC. For a given w/c ratio of 0.35, the concretes with HBC and OPC had shrinkage values of 0.0196% and 0.0230%, respectively. At the early stages of hydration, autogenous deformation of HBC concretes is much slower and less extensive. This lower autogenous shrinkage is attributed to the lower hydration of the HBC, which results in less mixing water being consumed. This finding also agrees with the compressive strength development because both autogenous shrinkage and strength development are remarkably affected by the hydration process of the cement used in the concrete [55]. Overall, the lower autogenous and drying shrinkage deformation of the concretes with HBC results from the low hydration

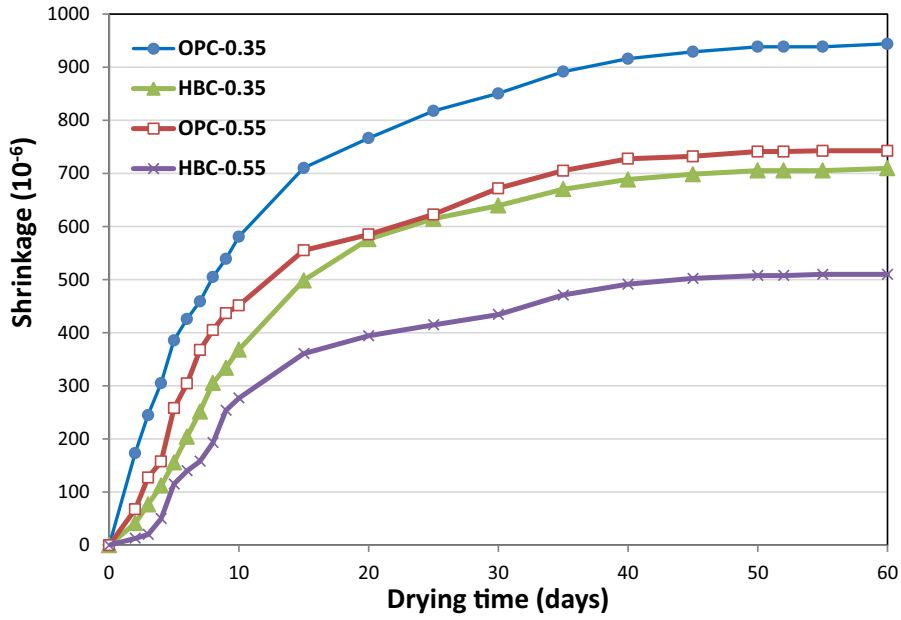

Fig. 9 Free shrinkage of the OPC-and HBC-concretes

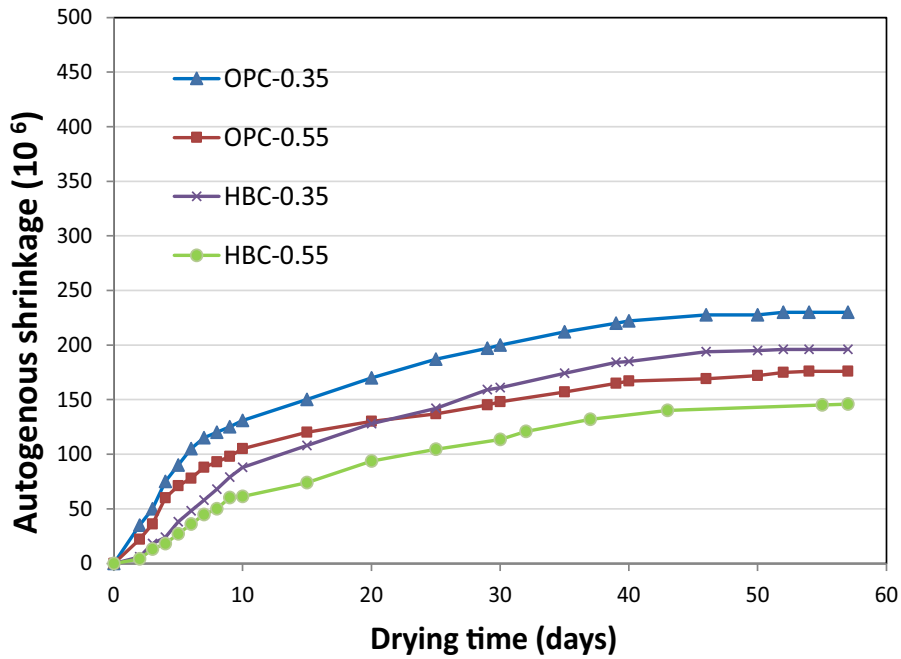

Fig. 10 Autogenous shrinkage of the OPC-and HBC-concretes

rate of the belite phase as well as the lack or small amount of the alite phase in the boron-modified cement. As mentioned by Saglik et al. [34], the main distinctive feature of HBC from OPC is the presence of a highly active belite phase instead of an alite phase. The hardening process of HBC concrete depends on the hydration of the active belite, while the other compounds seem to have minor roles.

When restrained, shrinkage strains make concrete more vulnerable to cracking since the tensile strength of concrete is quite low. Therefore, concrete is expected to crack immediately after the tensile stress induced by the constraint for the shrinkage strain beats

its tensile strength. As seen in Fig. 11, lower shrinkage deformations in the early ages also affected the restrained shrinkage cracking of the concretes. It is well known that the lower the early shrinkage, the longer the concrete cracking time will be. The effect of the lower shrinkage strain of the concretes with HBC was to prolong the cracking time of such concretes. Cracking was observed at 10 and 13 days of hydration for the HBC concretes with 0.35 and 0.55 w/c ratios, respectively, while OPC concretes experienced cracking at 6 and 10 days, respectively. Apart from the longer cracking time, using HBC influenced the crack propagation as well as the ultimate crack width of the concretes. Indeed, the crack opening was much faster in the case of OPC concretes, and the ultimate crack width was measured to be 1.1 and 0.9 mm at low and high w/c ratios, respectively. However, the concretes with HBC had 0.92 and 0.77 mm crack widths, respectively. Therefore, the lower values of drying shrinkage strain associated with lower heat of hydration and higher late strength of HBC give the concrete very good volume stability and thus much greater resistance to restrained shrinkage cracking [36]. On the other hand, higher drying shrinkage associated with higher elastic modulus and the prospective higher creep strains at the early ages helped in earlier cracking of OPC-based concretes despite its greater splitting tensile strength [49–52].

3.3 Resistance to water permeability and chloride ion ingress

Based on the physical–chemical phenomena, one of the most crucial issues causing concrete damage is water ingress with chloride and/or other aggressive ions into concrete. The microstructure of concrete controls this process and is associated with water transport and the ingress of ions into concrete [56].

Water penetration through capillary suction of the concretes with OPC and HBC is presented in terms of the sorptivity index in Fig. 12. This test is based on flowing water into the concrete through large connected pores, so it is considered a relative measure of the permeability. Figure 12 shows that there was a systematic decrease in the sorptivity with a prolonged curing period from 28 to 90 days, irrespective of the type of cement used. This effect was more influential in the case of HBC concretes because HBC had lower hydration kinetics than OPC [34, 36]. Indeed, the sorptivity index for the HBC-0.55 and OPC-0.55 concretes decreased from 0.231 to 0.170 and from 0.272 to 0.246 mm/min$^{1/2}$, respectively, with increasing curing period from 28 to 90 days. Such values indicated a 26% reduction for the former, while it was as low as 9% for the latter. At both the w/c ratio and curing age, the concretes with HBC had better performance against sorptivity than OPC-concretes. At 90 days, the reduction in the sorptivity of the concretes with the use of HBC was as high as 30%.

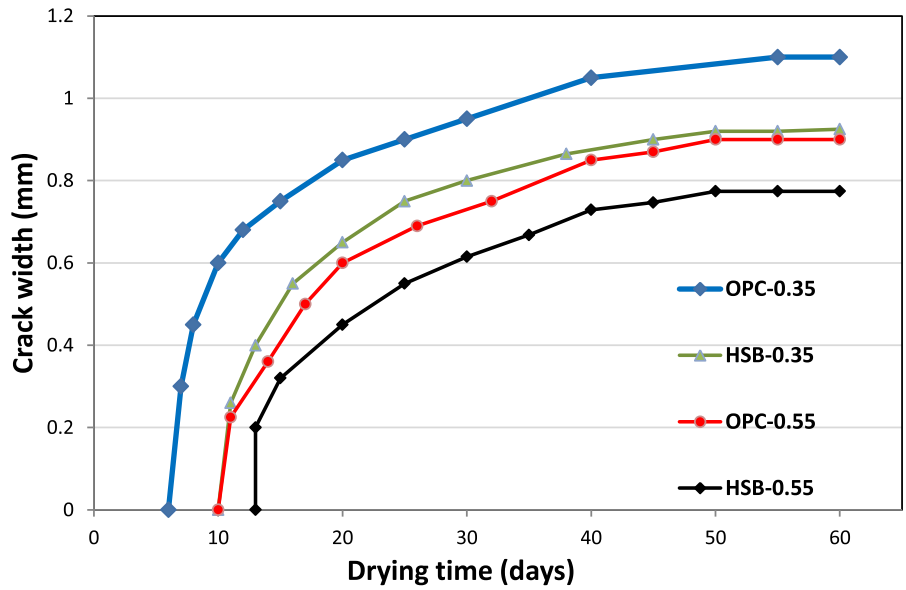

Fig. 11 Restrained shrinkage cracking of the OPC-and HBC-concretes

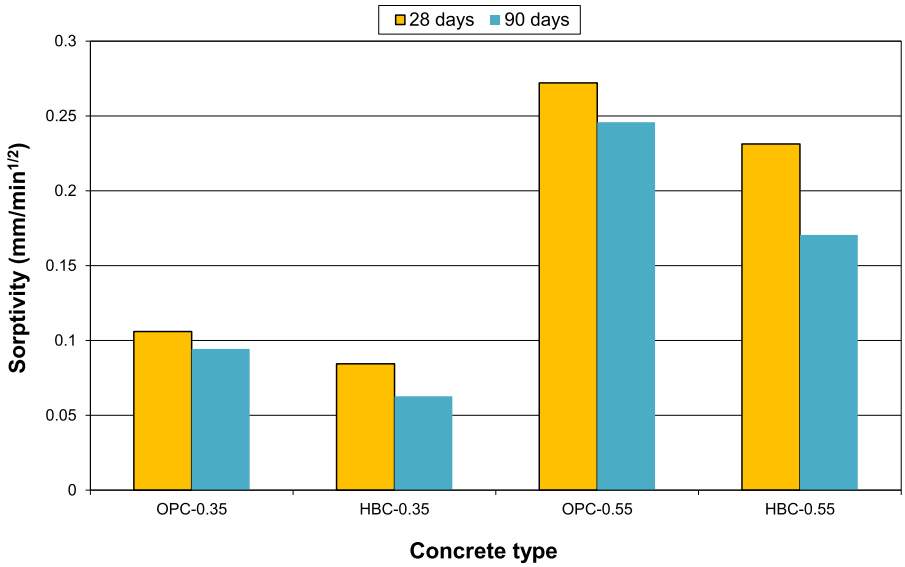

Fig. 12 Variation in the sorptivity of OPC- or HBC-concretes

Test results related to the resistance of the concretes against chloride ion penetration are presented in Fig. 13. The corresponding classification of the concretes as per ASTM C1202 [52] are given along the right-hand side of the figure. In line with the sorptivity index, when the concretes were made with HBC, they had considerable resistance to chloride ion ingress. At a low w/c ratio, the total charge values passed through the concretes with OPC were measured to be 1843 and 1643 C at 28 and 90 days, respectively, for which the rating of ASTM 1202 [52] was low. When HBC was introduced to the concrete, the total charge passed was reduced to 1545 and 1025 C at 28 and 90 days, respectively, corresponding to 16 and 38% decreases. Additionally, the corresponding ASTM classification shifted from low to very low at 90 days by using HBC in the concretes. Similarly, the concretes with HBC had higher resistance to chloride ion penetration at a high w/c ratio. Using HBC decreased the total charge from 5352 to 3526 C at 28 days and from 4271 to 2431 C at 90 days. Thus, HBC incorporation enhanced the concrete rating from high to moderate levels associated with 34 and 43% less total charge passing across the concretes at 28 and 90 days, respectively. The effect of a longer curing age on the performance of the concretes against chloride ion penetration was observed to be highly similar to the trend in the sorptivity. The concretes with HBC were much more improved with curing age than the OPC-concretes.

This behavior may be attributed to the fact that HBC has better pore refinement than OPC because the higher amount of C_2S in HBC compared to OPC led to a much lower amount of CH (calcium hydroxide). This is the weakest hydration product that mostly tends to gather in the interfacial transition zone between the aggregate and the matrix. It is well known that, when C_2S reacts with water, it generates a much lower content of CH than C_3S does. Moreover, there is a further hydration reaction at later ages to form additional tobermorite gel. Therefore, both the matrix itself and the interface between the aggregate and cement paste in HBC concretes have lower permeability, particularly at later ages, so the capillary water transport and chloride ion migration are much lower [34, 57, 58].

3.4 Resistance of concrete against corrosion-induced cracking

Previous studies have proven the accelerated corrosion test to be a successful measure to monitor the corrosion of steel bars embedded in concrete [59, 60]. Therefore, this test was employed to determine the resistance of the concretes with HBC and OPC against corrosion-induced cracking by applying a constant anodic potential. The current necessary to keep the fixed potential was plotted against time, as illustrated in Fig. 6b. Figure 6b shows that the

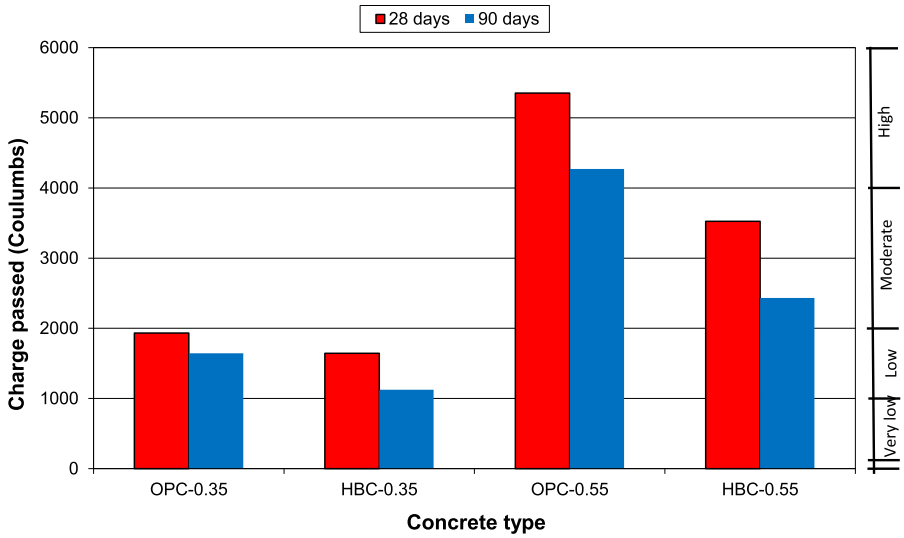

Fig. 13 Chloride ion permeability associated with the ASTM 1202 classifications of the concretes

current–time graph has an initial descending branch followed by a gradual ascending part. However, there will be a very sudden increase in the current attributed to the crack initiation induced by the corrosion expansion of the rebar. In addition to the inset of Figs. 6b and 14b shows the samples with damage due to corrosion of the rebar after the test was terminated. Moreover, a fast longitudinal crack is observed on the concrete specimens at the time of a sharp rise in the current.

Figure 14a shows the cracking time of the concretes with OPC and HBC due to the corrosion of steel bars. It was observed that the concretes with HBC had highly superior performance and mostly had a longer time to corrosion cracking compared to those with OPC. The corrosion resistance of HBC concretes increased remarkably from 28 to 90 days, whereas this increase was quite marginal in the case of OPC-included concretes. At a curing age of 28 days, for instance, first crack initiations on the concretes with OPC and HBC were observed at 115 and 149 and 92 and 108 h for the low and high w/c ratios, respectively. Such values indicated that using HBC in concrete production provided 30 and 17% later cracking ages, respectively. When the curing period was prolonged from 28 to 90 days, the concretes had longer times before corrosion cracking occurred. Thus, the time to failure for the HBC-0.35 concrete increased to 216 h, while that of the OPC-0.35 mixture extended to 143 h. The rise in the cracking age of the former was as high as 45% while that of the latter was approximately 24%. The outstanding performance of concrete with high belite cement is attributed to its intrinsic composition. In comparison to ordinary Portland cement, high belite cement has greater C_2S and lower C_3S and C_3A contents, thus resulting in much less calcium hydroxide (CH) and aluminum phases in its cement hydrates [61, 62]. It is commonly accepted that the gel of calcium silicate hydrates (CSH) formed by the hydration of C_2S has a higher polymerization degree. Therefore, the mineralogical characteristics of high belite cement result in denser hydration products with less calcium hydroxide and calcium aluminate hydrate, exhibiting a better resistance to deterioration by chloride attacks compared to Portland cement.

4 Conclusions

The following conclusions can be drawn according to the experimental results obtained in the current study.

(1) The early compressive strength of the concretes with HBC was lower than that of the OPC-based concretes, irrespective of the w/c ratio. However, after 7 days of curing, HBC-concrete exhibited a much better strength gain, resulting in a higher late compressive strength than OPC-concrete. Especially after a limiting curing age of 28 days, the compressive and splitting tensile strengths of the HBC-based concretes surpassed those of the concretes with OPC. The late compressive strength development of belite

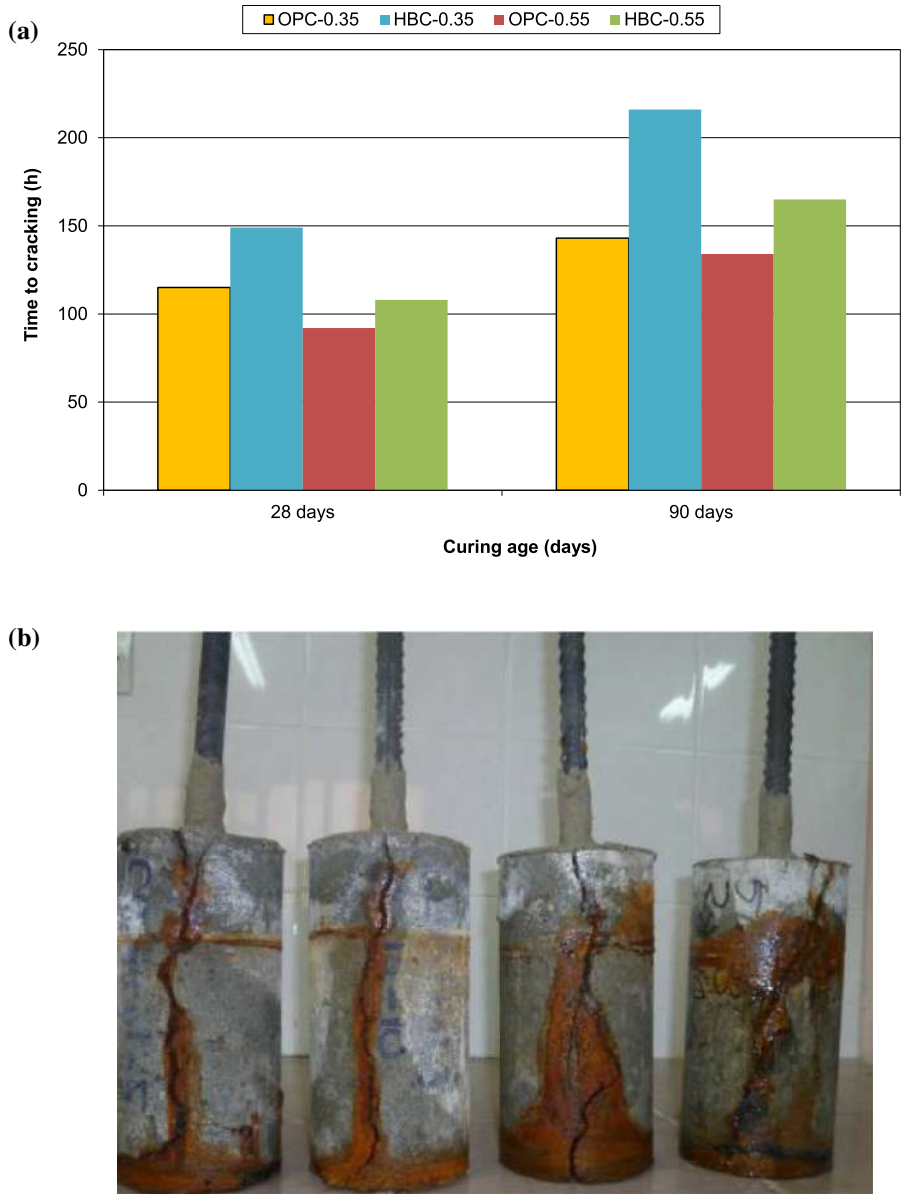

Fig. 14 **a** Average time to corrosion cracking **b** View of failed samples exposed to accelerated corrosion

cements depends mainly on the crystal type as well as the content of belite in the clinker. It was determined that the C_3S phase, formed at high ratios in normal Portland cement, did not form at all or formed in very small amounts in the BAB cement.

(2) Drying shrinkage of OPC-concrete exhibited a fast development rate, especially at early ages of hydration, and continued over the testing period. With the use of HBC, however, shrinkage at early ages showed a slower increase and led to much smaller ultimate shrinkage deformation. HBC-incorporated concretes also had much less autogenous shrinkage deformation than OPC-containing concretes. This lower autogenous shrinkage is attributed to the slower hydration of the HBC that results in less mixing water available to be consumed.

(3) The resistance of the concretes with HBC to restrained shrinkage cracking was beneficially

affected by the lower shrinkage deformations, which prolonged the cracking age. The crack width opening was much faster, leading to a wider ultimate crack in the case of OPC-concrete. The first crack on the OPC-concrete specimen was seen as early as on the 6^{th} day, which eventually reached 1.1 mm in width, while the HBC-concrete specimen cracked on the 10^{th} day, and the crack opening was only 0.92 mm. The lower values of drying and autogenous shrinkage associated with the lower heat of hydration and higher late strength of HBC give the concrete very good volume stability and thus much greater resistance to restrained shrinkage cracking.

(4) HBC-based concretes had remarkably lower sorptivity coefficients than the concretes with OPC, irrespective of testing age and curing conditions. This may be attributed to the higher amount of C_2S content in HBC compared to OPC, so that there is a further hydration reaction at later ages to form additional tobermorite gel. Moreover, the high C_2S content associated with the lack of C_3S gives rise to less calcium hydroxide, which generally accumulates in the cement paste-aggregate interfacial zone. Therefore, the resulting matrix as well as the matrix-aggregate interface become more compact with much lower porosity.

(5) The total charge values passed through the concretes with OPC were measured to be 1843 and 1643 C at 28 and 90 days, respectively, while those of HBC-concretes were 1545 and 1025 C at 28 and 90 days, respectively. Such values indicated reductions of 16 and 38% in the total charge passed. Additionally, the corresponding ASTM classification shifted from low to very low at 90 days when using HBC in the concretes. The reason for such an enhancement in the case of HBC concretes might be the more compact matrix and interface within the concrete structure in line with the sorptivity.

(6) It was observed that the concretes with HBC had highly superior performance and mostly featured a longer time to corrosion cracking when compared to those with OPC. The corrosion resistance of HBC concretes increased remarkably from 28 to 90 days, whereas this increase was quite marginal in the case of OPC-included concretes.

(7) High belite cement-based concretes seem to have better durability performance than OPC-concrete in many aspects owing to slow hydration associated with the denser matrix and interface structures.

Funding The authors have no financial or proprietary interests in any material discussed in this article.

Declarations

Conflict of interest The authors declare that they have no known competing financial interests or personal relationships that could have appeared to influence the work reported in this paper.

References

1. Cop26 Explained. UN Climate Change Conference UK 2021, Glasgow, 2021. https://ukcop26.org/wp-content/uploads/2021/11/COP26-Negotiations-Explained.pdf
2. Iacobescu RI, Koumpouri D, Pontikes Y, Saban R, Angelopoulos GN (2011) Valorisation of electric arc furnace steel slag as raw material for low energy belite cement. J Hazard Mater 196:287–294
3. Benhelal E, Zahedi G, Shamsaei E, Bahadori A (2013) Global strategies and potentials to curb CO_2 emissions in cement industry. J Clean Prod 51:142–161
4. Ishak SA, Hashim H (2015) Low carbon measures for cement plant-a review. J Clean Prod 103:260–274
5. Mehta PK (2002) Greening of the concrete industry for sustainable development. Concr Inter 24:23–28
6. Malhotra VM, Mehta PK (2002) High-performance, high-volume fly ash concrete: materials, mixture proportioning, properties, construction practice, and case histories. Supplementary Cementing Materials for Sustainable Development, Ottawa, Canada
7. Damtoft JS, Lukasik J, Herfort D, Sorrentino D, Gartner EM (2008) Sustainable development and climate change initiatives. Cem Concr Res 38(2):115–127
8. Gartner E (2004) Industrially interesting approaches to low CO_2 cements. Cem Concr Res 34(9):1489–1498
9. Saidur R, Rahim NA, Hasanuzzaman M (2010) A review on compressed air energy use and energy savings. Renew Sustain Energy Rev 14:1135–1153
10. Singhi MK, Bhargava R (2010) Sustainable Indian cement industry, in: Workshop on International Comparison of Industrial Energy Efficiency. http:// www.beeindia.in/seminars/document/2010/R.%20bha.pdf
11. Guerrero A, Goni S, Macias A, Luxan MP (1999) Hydraulic activity and microstructural characterization of new fly ash-belite cements synthesized at different temperatures. J Mater Res 14(6):2680–2687

12. Guerrero A, Goni S, Campillo I, Moragues A (2004) Belite cement clinker from coal fly ash of high Ca content: optimization of synthesis parameters. Environ Sci Technol 38(11):3209–3213
13. Chatterjee AK (1996) High belite cements. Present status and future technological options: Part I and Part II. Cem Concr Res 26(8):1213–1237
14. De la Torre AG, Aranda MAG, De Aza AH, Pena P, De Aza S (2005) Belite portland clinkers. Synthesis and mineralogical analysis. Bol Soc Esp Ceram Vidr 44(3):185–191
15. Kacimi L, Simon-Masseron A, Salem S, Ghomari A, Derriche Z (2009) Synthesis of belite cement clinker of high hydraulic reactivity. Cem Concr Res 39:555–565
16. Cuberos AJM, De La Torre AG, Martín-Sedeño MC, Moreno-Real L, Merlini M, Ordónez LM, Aranda MAG (2009) Phase development in conventional and active belite cement pastes by Rietveld analysis and chemical constraints. Cem Concr Res 39:883–842
17. Martín-Sedeño MC, Cuberos AJM, De la Torre AG, Pinazo GA, Ordónez LM, Gateshki M, Aranda MAG (2010) Aluminum-rich belite sulfoaluminate cements: clinkering and early age hydration. Cem Concr Res 40:359–369
18. Londono-Zuluaga D, Tobon JI, Aranda MAG, Santacruz I, De la Torre AG (2017) Clinkering and hydration of belite-alite-yeelimite cement. Cem Concr Compos 80:333–341
19. Popescu CD, Muntean M, Sharp JH (2003) Industrial trial production of low energy belite cement. Cem Concr Compos 25(7):689–693
20. Cuesta A, Ayuela A, Aranda MGA (2021) Belite cements and their activation. Cem Concr Res 140:106319
21. Turk S, Gurbuz G, Ertun T, Yeginobali A (2006) Heat of hydration and shrinkage properties of Boron containing active belite cements. ConcreteLife'06 - International RILEM-JCI Seminar on Concrete Durability and Service Life Planning: Curing, Crack Control, Performance in Harsh Environments, RILEM Publications SARL, pp 397–404
22. El-Didamony H, Sharara AM, Helmy IM, El-Aleem SA (1996) Hydration characteristics of β-C_2S in the presence of some accelerators. Cem Concr Res 26:1179–1187
23. Campillo I, Guerrero A, Dolado JS, Porro A, Ibanez JA, Goni S (2007) Improvement of initial mechanical strength by nanoalumina in belite cements. Mater Lett 61:1889–1892
24. Jang JG, Lee HK (2016) Microstructural densification and CO_2 uptake promoted by the carbonation curing of belite-rich Portland cement. Cem Concr Res 82:50–57
25. Ibanez J, Artús L, Cusco R, Lopez A, Menendez E, Andrade MC (2007) Hydration and carbonation of monoclinic C_2S and C_3S studied by Raman spectroscopy. J Raman Spectrosc 38:61–67
26. Fang Y, Chang J (2017) Rapid hardening β-C_2S mineral and microstructure changes activated by accelerated carbonation curing. J Therm Anal 129:681–689
27. Sakai E, Nakajima K, Kubokawa T, Sotokawa S, Daimon M (2010) Polymer-modified cement using belite-rich cement and carbonation reaction. Constr Build Mater 110:333–336
28. Gosh SN, Rao PB, Paul AK, Raina K (1979) The chemistry of dicalcium silicate mineral. J Mater Sci 14:1554–1556
29. Butt YM, Timashev VV, Malozohn LI (1968) In: Proceedings of the 5th International Symposium on the Chemistry of Cement 1, Cement Association of Japan Tokyo, p 340
30. Lawrence CD (2003) The production of low-energy cements. Lea's chemistry of cement and concrete. Butterworth-Heinemann, Oxford
31. Kim YJ, Nettleship I, Kriven WM (1992) Phase transformations in dicalcium silicate. II: TEM studies of crystallography, microstructures and mechanisms. J Am Ceram Soc 75:2407–2419
32. Engstrom F, Pontikes Y, Geysen D, Jones PT, Björkman B, Blanpain B (2011) Review: hot stage engineering to improve slag valorisation options. In: Proceedings 2nd international slag valorisation symposium, Leuven
33. Koumpouri D, Angelopoulos GN (2016) Effect of boron waste and boric acid addition on the production of low energy belite cement. Cem Concr Compos 68:1–8
34. Saglik A, Sümer O, Tunc E, Kocabeyler MF, Celik RS (2008) The characteristics of boron modified active belite (BAB) cement and its utilization in mass and conventional concrete. In: Proceedings 11DBMC international conference on durability of building materials and components, Istanbul Turkey
35. Sirtolia D, Wyrzykowski M, Riva P, Tortelli S, Marchi M, Lurab P (2019) Shrinkage and creep of high-performance concrete based on calcium sulfoaluminate cement. Cem Concr Compos 98:61–73
36. Sui T, Fan L, Wen Z, Wang J, Zhang Z (2004) Study on the properties of high strength concrete using high belite cement. J Adv Concr Tech 2(2):201–206
37. Afroughsabet V, Biolzi L, Monteiro PJM, Gastaldi MM (2021) Investigation of mechanical and durability properties of sustainable high performance concrete based on calcium sulfoaluminete cement. J Build Eng 43:102656
38. Guerrero A, Goni S, Macias A (2000) Durability of new fly ash±belite cement mortars in sulfated and chloride medium. Cem Concr Res 30:1231–1238
39. Gokce HS (2019) High temperature resistance of boron active belite cement mortars containing fly ash. J Cleaner Prod 211:992–1000
40. Shi X, Xie N, Fortune K, Gong J (2012) Durability of steel reinforced concrete in chloride environments: an overview. Constr Build Mater 30:125–138
41. Saglik A (2019) The characteristics of boron modified active belite (BAB) cement. In: Proceedings 15th international congress on chemistry of cement, Prague, Czech Republic, p 1644–1654
42. Irico S, Mutke S, Bertola F, Gastaldi D, Capelli L, Canonico F (2022) Durability of high belite cement as new technical solution for concrete. Acta Polytech CTU Proc 33:245–249
43. Irico S, Qvaeschning D, Mutke S, Deuse T, Gastaldi D, Canonico F (2021) Durability of high performance self-compacting concrete with granulometrically optimized slag cement. Constr Build Mater 298:123836
44. TS EN 197–1 (2002) Cement- Part 1: compositions and conformity criteria for common cements, Turkish Standards, March 2002
45. ASTM C39 (2012) Standard test method for compressive strength of cylindrical concrete specimens. In: Annual Book of ASTM Standard, 2012

46. ASTM C496 (2011) Standard test method for splitting tensile strength of cylindrical concrete specimens. In: Annual Book of ASTM Standard, 2011
47. ASTM C157 (2007) Standard test method for length change of hardened hydraulic-cement mortar and concrete. Annual Book of ASTM Standards
48. Wiegrink K, Marikunte SM, Shah SP (1996) Shrinkage cracking of highstrength concrete. ACI Mater J 93(5):409–415
49. Grzybowski M, Shah SP (1990) Shrinkage cracking of fiber reinforced concrete. ACI Mater J 87(2):138–148
50. Shah SP, Karaguler ME, Sarigaphuti M (1992) Effects of shrinkage-reducing admixtures on restrained shrinkage cracking of concrete. ACI Mater J 89(3):289–295
51. Sarigaphuti M, Shah SP, Vinson KD (1993) Shrinkage cracking and durability characteristics of cellulose fiber reinforced concrete. ACI Mater J 90(4):309–318
52. ASTM C1202 (2006) Test method for electrical indication of concrete's ability to resist chloride ion penetration. In: Annual Book of ASTM Standards, American Society for Testing and Materials, V. 4.02
53. Brooks JJ (2015) Methods of predicting elasticity. Shrinkage And Creep Of Concrete, Concrete and Masonry Movements
54. Gribniak V (2008) Shrinkage in reinforced concrete structures: a computional aspect, Dept. of Bridges and Special Structure, Vilnius Gediminas Technical University, Lithuania
55. Yeung JSK, Yam MCH, Wong YL (2020) Model for predicting shrinkage of concrete using calcium sulfoaluminate cement blended with OPC. PFA and GGBS J Build Eng 32:101671
56. Bh O, Cha SW, Jang BS, Jang SY (2002) Development of high-performance concrete having high resistance to chloride penetration. Nucl Eng Des 212:221–231
57. Guerrero A, Goni S, Moragues A, Dolado JS (2005) Microstructure and mechanical performance of belite cements from high calcium coal fly ash. J Am Ceramic Soc 88:1845–1853
58. Poon CS, Kou SC, Lam L (2006) Compressive strength, chloride diffusivity, and pore structure of high performance metakaolin and silica fume concrete. Constr Build Mater 20:858–865
59. Al-Zahani MM, Al-Dulaijan SU, Ibrahim M, Saricimen H, Sharif FM (2002) Effect of waterproofing coating on steel reinforcement corrosion and physical properties of concrete. Cement Concrete Compos 24:127–137
60. Guneyisi E, Ozturan T, Gesoglu M (2005) A study on reinforcement corrosion and related properties of plain and blended cement concretes under different curing conditions. Cement Concrete Compos 27:449–461
61. Jiang C, Jiang L, Li S, Tang X, Zhang L (2021) Impact of cation type and fly ash on deterioration process of high belite cement pastes exposed to sulfate attack. Constr Build Mater 286:122961
62. Jiang C, Yu L, Tang X, Chu H, Jiang L (2021) Deterioration process of high belite cement paste exposed to sulfate attack, calcium leaching and the dual actions. J Mater Res Tech 15:2982–2992